Magazine of Civil Engineering. 2019. 87(3). Pp. 66–79
Инженерно-строительный журнал. 2019. № 3(87). С. 66–79

Magazine of Civil Engineering

ISSN 2071-0305

journal homepage: http://engstroy.spbstu.ru/

DOI: 10.18720/MCE.87.6

The semi-shear theory of V.I. Slivker for the stability problems of thin-walled bars

V.V. Lalin, V.A. Rybakov, S.F. Diakov, V.V. Kudinov, E.S. Orlova*,
Peter the Great St. Petersburg Polytechnic University, St. Petersburg, Russia
** E-mail: ye-cat-erina@yandex.ru*

Keywords: stability, geometric stiffness matrix, thin-walled bar, finite element method, semi-shear theory.

Abstract. The theory of thin-walled bars is important because light steel thin-walled structures are widely used. Traditionally, in calculations two theories are used: theory for open-profile and closed profile bars. The calculations are difficult, because different finite elements are used for different bar types. In 2005 V.I. Slivker worked out a semi-shear theory, which is suitable for thin-walled bars of open sections and closed sections. Similarly, this article presents the research on finite element modeling for the stability problems of thin-walled bars using the same theory to the geometric stiffness matrix. It was shown that the FEM solution converges to the exact one as the number of the finite elements increases. The numeral solutions were compared to critical forces obtained by the classical Euler formula. It was found that using the cross-sections as the thin-walled ones can reduce the critical force, especially for the open cross-sections.

1. Introduction

The importance of the theory of thin-walled [1, 2] for structural analysis [3] bars has significantly increased both in Russia [4] and abroad during the last years. This theory has such advantages as prefabrication and lightness of elements, which are analyzed in articles of Russian and foreign researchers. In these articles the calculations of stress strain state [5, 6], strength [7] and stability of thin-walled bars [8, 9] are quoted.

The problems of stress strain state and stability of bars can be accurately solved by using of plate or volume finite elements, due to technical complexity this method cannot find wide practical application.

The buckling of thin-walled bars was investigated by G.I. Bely [10, 11]. In his articles some characteristics of steel galvanized bars were considered. As a result an algorithm for determination of the most suitable cross-section parameters was presented. The parameters depend on the flexibility of the structures.

The problem of stability is so difficult that sometimes it is necessary to use experimental methods [12, 13].

The theory of thin-walled bars, which was developed by V.Z. Vlasov, is one of the first fundamental method to solve a problem of stability. This theory is suitable for open profile bars. At the same years A.A. Umanskiy developed the thin-walled theory for closed profile bars, which has some differences from Vlasov theory in mathematical apparatus. Both theories have joint properties, such as bimoment and warping effect, which are additional force factor and deformation. At the same time other Russian scientists [14, 15] published works repeating and complementaring these two problems.

With the development of the finite element method (FEM), some scientists tried to establish a thin-walled theory, which are more suitable in practice than Umanskiy theory [16, 17]. The problem of thin-walled stability is researched by foreign scientists. They analyze the problem of plane [18, 19] and spatial buckling [20, 21] for bearing elements and angle stiffeners of buildings [22, 23], for permanent and dynamic loads. Also there are some articles about stability of rods on cushion course [24].

Lalin, V.V., Rybakov, V.A., Diakov, S.F., Kudinov, V.V., Orlova, E.S. The semi-shear theory of V.I. Slivker for the stability problems of thin-walled bars. Magazine of Civil Engineering. 2019. 87(3). Pp. 66–79. DOI: 10.18720/MCE.87.6

Лалин В.В., Рыбаков В.А., Дьяков С.Ф., Кудинов В.В., Орлова Е.С. Полусдвиговая теория В.И. Сливкера в задачах устойчивости тонкостенных стержней // Инженерно-строительный журнал. 2019. № 3(87). С. 66–79. DOI: 10.18720/MCE.87.6

In [25] it is shown how to get stiffness matrix for binodal finite element, which has seven degrees of freedom in each node. Author applied this matrix for solving dynamic problems. The matrix was obtained without taking into account that the assumption that the angles of rotation are small.

The buckling of bars can be treated as general buckling and wrinkling. The modes of buckling were analyzed in the works of Askinazi V.U. After detailed evaluation of modes of buckling (torsional, bending and bending-torsional modes) it is concluded that modes of buckling depend on bars characteristics such as stiffness, pitch and others.

However V.I. Slivker used only Lagrangian and stability functionals. It means, this topic can be developed in future. Authors of this article applied special finite elements for solving static [26] and dynamic [27] problems.

The semi-shear theory of V.I. Slivker [28] has some advantages in comparison with Vlasov and Umanskiy theory. The Slivker theory allows using one analytical model for bars of opened and closed profile, so it is more suitable in practice.

In the semi-shear theory the shear deformations are taken into account, which leads to more accurate solution. The main tangential stresses in the semi-shear theory are torsional stresses, while bending stresses are considered secondary. The shape of cross-section of bars is considered by shape coefficient.

In this article authors use FEM according to Slivker theory to solve stability problems of thin-walled elements. The process incorporates the following stages:

1) the stiffness matrix and the geometrical stiffness matrix are constructed;
2) critical force for different cross-section types (open-profile and closed profile bars) is estimated;
3) critical force for thin-walled rods and Euler's critical force are compared;
4) the recommendations are given in which cases the cross-section should be used as a thin-walled.

2. Methods

Let us consider a coordinate system (X, Y, Z) – a right-handed Cartesian system where an axis X matches an axial axis of the bar passing the center of gravity. Axes Y and Z are the main central axes of inertia of the bar.

Equilibrium stability functional for the beam column bar within the semi-shear theory can be written as follows:

$$S=\frac{1}{2}\int_0^L[GI_x\theta'^2+GI_\beta(\theta'-\beta)^2+EI_z\eta''^2+EI_y\zeta''^2+EI_\omega\beta'^2+K\theta'^2+N(\eta'^2+\zeta'^2)+ \\ +2(M_\eta\eta''-M_\zeta\zeta'')\theta]dx, \tag{1}$$

where L is length of the thin-walled bar,

θ is angle of torsion,

β is warping measure function,

η is shear center displacement with respect to the Y axis,

ξ is shear center displacement with respect to the Z axis,

η' is angle of rotation with respect to the Z axis,

ξ' is angle of rotation with respect to the Y axis,

E is Young's modulus,

G is shear modulus:

$$G=\frac{E}{2(1+v)'} \tag{2}$$

v is Poisson's ratio,

I_x is torsional moment of inertia,

I_β is warping moment of inertia:

$$I_\beta = \frac{I_r}{\mu_{\omega\omega}} \tag{3}$$

I_r is polar moment of inertia:

$$I_r = I_z + I_y \tag{4}$$

I_z, I_y are moments of inertia about the axes Z and Y,

$\mu_{\omega\omega}$ is a cross-section form coefficient:

$$\mu_{\omega\omega} = \frac{I_r}{I_\omega^2}\int_\Omega \frac{S_{o\omega}^2}{t}ds \tag{5}$$

I_ω is sectorial moment of inertia,

Ω is a cross-section profile length,

t is wall thickness of the bar,

$S_{o\omega}^2$ is sectorial static moment of the cut-off part of the cross-section,

N is normal force in the bar, which is considered to be positive in case of bar extension.

K, M_η, M_ζ are characteristics which depend on the internal force factors.

$$K = Nr_p^2 + M_y b_z + M_z b_y + Bb_\omega,\ \ M_\eta = M_y - Nz_p, M_\zeta = M_z - Ny_p \tag{6}$$

M_y is bending moment about the Y-axis is assumed to be positive if it causes tension in fibers with positive coordinate z.

M_z is bending moment about the Z-axis is assumed to be positive if it causes tension in fibers with positive coordinate y.

B is bimoment is assumed to be positive if it causes tension in points of the bar which have a positive sectorial coordinate ω.

y_p, z_p is coordinates of the bending center in the Cartesian system (axes Y, Z)

r_p is polar radius of inertia of the bar's cross-section about the bending center:

$$r_p^2 = \frac{I_r}{A} + y_p^2 + z_p^2. \tag{7}$$

A is cross-section area,

b_z, b_y, b_ω are geometrical parameters of the cross section:

$$b_z = \frac{J_{zzz} + J_{yyz}}{I_y} - 2z_p,\ \ b_y = \frac{J_{yyy} + J_{yzz}}{I_z} - 2y_p,\ \ b_\omega = \frac{J_{yy\omega} + J_{zz\omega}}{I_\omega} \tag{8}$$

$J_{zzz}, J_{yyz}, J_{yyy}, J_{yzz}, J_{yy\omega}, J_{zz\omega}$ are moments of inertia of the third order:

$$\begin{gathered} J_{zzz} = \int_\Omega z^3 hds,\ \ J_{yyz} = \int_\Omega y^2 zhds,\ \ J_{yyy} = \int_\Omega y^3 hds,\ \ J_{yzz} = \int_\Omega yz^2 hds, \\ J_{yy\omega} = \int_\Omega y^2 \omega hds,\ \ J_{zz\omega} = \int_\Omega z^2 \omega hds. \end{gathered} \tag{9}$$

Let us divide L-length thin-walled bar into n two-node finite elements. Then, i-th finite element, having length l, nodes i and i+1 and 6 degrees of freedom will look like:

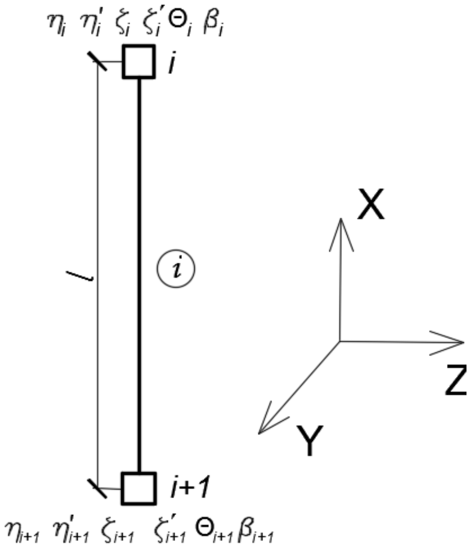

Figure 1. The two-node finite element with twelve degrees of freedom.

$$[U]^T = (\eta_i, \eta_i^{'}, \zeta_i, \zeta_i^{'}, \theta_i, \beta_i, \eta_{i+1}, \eta_{i+1}^{'}, \zeta_{i+1}, \zeta_{i+1}^{'}, \theta_{i+1}, \beta_{i+1})\,. \quad (10)$$

Column of node displacements of the finite element is:

To use FEM within the theory of thin-walled bars functions of the transverse displacements $\eta(x)$ и $\zeta(x)$ should be represented with the Hermite polynomials H_j:

$$\eta(x) = H_1\eta_i + H_2\eta_i^{'} + H_3\eta_{i+1} + H_4\eta_{i+1}^{'}\,,$$
$$\zeta(x) = H_1\zeta_i + H_2\zeta_i^{'} + H_3\zeta_{i+1} + H_4\zeta_{i+1}^{'}\,. \quad (11)$$

As the functions η и ξ in functional (1) have derivatives of order at most second, they should be approximated by the cubic functions.

Hermite polynomials look like this:

$$H_1(x) = \frac{2}{l^3}x^3 - \frac{3}{l^2}x^3 + 1,\ \ H_2(x) = \frac{1}{l^2}x^3 - \frac{2}{l}x^2 + x,$$
$$H_3(x) = \frac{-2}{l^3}x^3 + \frac{3}{l^2}x^2,\ H_4(x) = \frac{1}{l^2}x^3 - \frac{1}{l}x^2. \quad (12)$$

Let us write equation (11) in the matrix form in order to represent functional (1) in the matrix view.

$$\eta(x) = [H]_{\eta\zeta}[U_\eta],\ \ \zeta(x) = [H]_{\eta\zeta}[U_\zeta]\,, \quad (13)$$

where $[H]_{\eta\zeta}$ is row-matrix made of four Hermite polynomials:

$$[H]_{\eta\zeta} = [H_1(x),\ \ H_2(x),\ \ H_3(x),\ \ H_4(x)]\,, \quad (14)$$

$[U_\eta],\ [U_\zeta]$ are node displacement columns.

$$[U_\eta]^T = (\eta_{i,}\ \ \ \eta_i^{'},\ \ \eta_{i+1},\ \ \eta_{i+1}^{'})\,,$$
$$\left[U_\zeta\right]^T = \left(\zeta_i,\ \zeta_i',\ \zeta_{i+1},\ \zeta_{i+1}'\right). \quad (15)$$

Then:

$$(\eta^{'})^2 = ([H^{'}]_{\eta\zeta}[U_\eta])^2 = ([H^{'}]_{\eta\zeta}[U_\eta])^T([H^{'}]_{\eta\zeta}[U_\eta]) = [U_\eta]^T[H^{'}]_{\eta\zeta}^T[H^{'}]_{\eta\zeta}[U_\eta] \quad (16)$$

Similarly:

$$(\eta'')^2 = [U_\eta]^T [H'']^T_{\eta\zeta} [H'']_{\eta\zeta} [U_\eta],$$
$$(\zeta')^2 = [U_\zeta]^T [H']^T_{\eta\zeta} [H']_{\eta\zeta} [U_\zeta], \quad (17)$$
$$(\zeta'')^2 = [U_\zeta]^T [H'']^T_{\eta\zeta} [H'']_{\eta\zeta} [U_\zeta].$$

where

$$[H']_{\eta\zeta} = \left[\frac{dH_1(x)}{dx}, \frac{dH_2(x)}{dx}, \frac{dH_3(x)}{dx}, \frac{dH_4(x)}{dx}\right],$$
$$[H'']_{\eta\zeta} = \left[\frac{d^2H_1(x)}{dx^2}, \frac{d^2H_2(x)}{dx^2}, \frac{d^2H_3(x)}{dx^2}, \frac{d^2H_4(x)}{dx^2}\right]. \quad (18)$$

Let us represent functions $\theta(x)$ и $\beta(x)$ as a sum of products of linear polynomials and node displacements, as in functional (1) they have derivatives of order at most first.

$$\theta(x) = H_5\theta_i + H_6\theta_{i+1},$$
$$\beta(x) = H_5\beta_i + H_6\beta_{i+1}. \quad (19)$$

The polynomials are:

$$H_5(x) = -\frac{1}{l}x + 1, \quad H_6(x) = \frac{1}{l}x. \quad (20)$$

In matrix form for formulas (19) is:

$$\theta(x) = [H]_{\theta\beta}[U_\theta],$$
$$\beta(x) = [H]_{\theta\beta}[U_\beta], \quad (21)$$

where

$$[H]_{\theta\beta} = [H_5(x), \;\; H_6(x)], \quad (22)$$

$$[U_\theta]^T = (\theta_i, \;\; \theta_{i+1}),$$
$$[U_\beta]^T = (\beta_i, \;\; \beta_{i+1}). \quad (23)$$

Then:

$$(\theta')^2 = [U_\theta]^T [H']^T_{\theta\beta} [H']_{\theta\beta} [U_\theta],$$
$$(\beta')^2 = [U_\beta]^T [H']^T_{\theta\beta} [H']_{\theta\beta} [U_\beta], \quad (24)$$

where

$$[H']_{\theta\beta} = \left[\frac{dH_5(x)}{dx}, \frac{dH_6(x)}{dx}\right]. \quad (25)$$

Difference $(\theta' - \beta)$ will be:

$$\theta'(x) - \beta(x) = [\Phi][U_{\theta\beta}], \quad (26)$$

where

$$[\Phi] = \left(\frac{dH_5(x)}{dx}, -H_5(x), \frac{dH_6(x)}{dx}, -H_6(x)\right), \quad (27)$$

$$[U_{\theta\beta}]^T = (\theta_i, \;\; \beta_i, \;\; \theta_{i+1}, \;\; \beta_{i+1}), \quad (28)$$

$$(\theta'(x) - \beta(x))^2 = [U_{\theta\beta}]^T [\Phi]^T [\Phi][U_{\theta\beta}]. \quad (29)$$

To make the geometric stiffness matrix symmetric an item $2(M_\eta\eta'' - M_\zeta\zeta'')\theta$ can be expanded as follows:

$$
\begin{aligned}
&2(M_\eta\eta'' - M_\zeta\zeta'')\theta = 2M_\eta\eta''\theta - 2M_\zeta\zeta''\theta = 2M_\eta\left(\frac{1}{2}\eta''\theta + \frac{1}{2}\theta\eta''\right) - \\
&- 2M_\zeta\left(\frac{1}{2}\zeta''\theta + \frac{1}{2}\theta\zeta''\right) = M_\eta(\eta''\theta + \theta\eta'') - M_\zeta(\zeta''\theta + \theta\zeta'') = \\
&= M_\eta([U_\eta]^T[H'']^T_{\eta\zeta}[H]_{\theta\beta}[U_\theta] + [U\theta]^T[H]^T_{\theta\beta}[H'']_{\eta\zeta}[U_\eta] - \\
&- M_\zeta([U_\zeta]^T[H'']^T_{\eta\zeta}[H]_{\theta\beta}[U_\theta] + [U_\theta]^T[H]^T_{\theta\beta}[H'']_{\eta\zeta}[U_\zeta])].
\end{aligned}
\tag{30}
$$

Using (16), (17), (24), (29) и (30) the functional (1) will be:

$$
\begin{aligned}
S = \frac{1}{2}\int_0^L &[GI_x[U_\theta]^T[H']^T_{\theta\beta}[H']_{\theta\beta}[U_\theta] + GI_\beta[U_{\theta\beta}]^T[\Phi]^T[\Phi][U_{\theta\beta}] + \\
&+ EI_z[U_\eta]^T[H'']^T_{\eta\zeta}[H'']_{\eta\zeta}[U_\eta] + EI_y[U_\zeta]^T[H'']^T_{\eta\zeta}[H'']_{\eta\zeta}[U_\zeta] + \\
&+ EI_\omega[U_\beta]^T[H']^T_{\theta\beta}[H']_{\theta\beta}[U_\beta] + K[U_\theta]^T[H']^T_{\theta\beta}[H']_{\theta\beta}[U_\theta] + \\
&+ N([U_\eta]^T[H']^T_{\eta\zeta}[H']_{\eta\zeta}[U_\eta] + [U_\zeta]^T[H']^T_{\eta\zeta}[H']_{\eta\zeta}[U_\zeta]) + \\
&+ M_\eta([U_\eta]^T[H'']^T_{\eta\zeta}[H]_{\theta\beta}[U_\theta] + [U_\theta]^T[H]^T_{\theta\beta}[H'']_{\eta\zeta}[U_\eta]) - \\
&- M_\zeta([U_\zeta]^T[H'']^T_{\eta\zeta}[H]_{\theta\beta}[U_\theta] + [U_\theta]^T[H]^T_{\theta\beta}[H'']_{\eta\zeta}[U_\zeta])]dx.
\end{aligned}
\tag{31}
$$

Let us consider P as the concentrated load applied along the axis X on the end of the bar at any point of the cross-section A, which has coordinates $(e_y,\ e_z)$ about the axes Y, Z. As the result, regarding the accepted rules of signs, we will get:

$$
N = -P, \quad M_y = -Pe_z, \quad M_z = -Pe_y, \quad B = -P\omega_A,
\tag{32}
$$

where ω_A sectorial coordinate of the point A where load P is applied.

Using (32) we can write (6) as follows:

$$
\begin{gathered}
K = Nr_p^2 + M_y b_z + M_z b_y + Bb_\omega = -\Pr_p^2 - Pe_z b_z - Pe_y b_y - P\omega_A b_\omega = \\
= -P(r_p^2 + e_z b_z + e_y b_y + \omega_A b_\omega), \\
M_\eta = M_y - Nz_p = -Pe_z + Pz_p = -P(e_z - z_p), \\
M_\zeta = M_z - Ny_p = -Pe_y + Py_p = -P(e_y - y_p)
\end{gathered}
\tag{33}
$$

Using (33) functional (31) can be written:

$$
\begin{aligned}
S = \frac{1}{2}\int_0^L &\{GI_x[U_\theta]^T[H']^T_{\theta\beta}[H']_{\theta\beta}[U_\theta] + GI_\beta[U_{\theta\beta}]^T[\Phi]^T[\Phi][U_{\theta\beta}] + \\
&+ EI_z[U_\eta]^T[H'']^T_{\eta\zeta}[H'']_{\eta\zeta}[U_\eta] + EI_y[U_\zeta]^T[H'']^T_{\eta\zeta}[H'']_{\eta\zeta}[U_\zeta] + \\
&+ EI_\omega[U_\beta]^T[H']^T_{\theta\beta}[H']_{\theta\beta}[U_\beta] - P[(r_p^2 + e_z b_z + e_y b_y + \omega_A b_\omega)[U_\theta]^T[H']^T_{\theta\beta} \\
&[H']_{\theta\beta}[U_\theta] + [U_\eta]^T[H']^T_{\eta\zeta}[H']_{\eta\zeta}[U_\eta] + [U_\zeta]^T[H']^T_{\eta\zeta}[H']_{\eta\zeta}[U_\zeta] + \\
&+ (e_z - z_p)([U_\eta]^T[H'']^T_{\eta\zeta}[H]_{\theta\beta}[U_\theta] + [U_\theta]^T[H]^T_{\theta\beta}[H'']_{\eta\zeta}[U_\eta] - \\
&- (e_y - y_p)([U_\zeta]^T[H'']^T_{\eta\zeta}[H]_{\theta\beta}[U_\theta] + [U_\theta]^T[H]^T_{\theta\beta}[H'']_{\eta\zeta}[U_\zeta]\}dx
\end{aligned}
\tag{34}
$$

Estimating integrals and putting the results together according to the nodal displacements' indexing in (10) equation (34) will be:

$$S = \frac{1}{2}[U]^T([K] - P[G])[U], \tag{35}$$

where $[U]$ is a column of nodal displacements from equation (10),

$[K]$ is stiffness matrix,

$[G]$ is geometric stiffness matrix.

Matrixes $[K]$and $[G]$ are:

$$[K] = \begin{pmatrix} K_{11} & K_{12} \\ K_{21} & K_{22} \end{pmatrix}, \quad [G] = \begin{pmatrix} G_{11} & G_{12} \\ G_{21} & G_{22} \end{pmatrix}. \tag{36}$$

where

$$K_{11} = \begin{pmatrix} \frac{12}{l^3}EI_z & \frac{6}{l^2}EI_z & 0 & 0 & 0 & 0 \\ \frac{6}{l^2}EI_z & \frac{4}{l}EI_z & 0 & 0 & 0 & 0 \\ 0 & 0 & \frac{12}{l^3}EI_y & \frac{6}{l^2}EI_y & 0 & 0 \\ 0 & 0 & \frac{6}{l^2}EI_y & \frac{4}{l}EI_y & 0 & 0 \\ 0 & 0 & 0 & 0 & \frac{1}{l}GI_x + \frac{1}{l}GI_\beta & \frac{1}{2}GI_\beta \\ 0 & 0 & 0 & 0 & \frac{1}{2}GI_\beta & \frac{l}{3}GI_\beta + \frac{1}{l}EI_\omega \end{pmatrix},$$

$$K_{12} = \begin{pmatrix} -\frac{12}{l^3}EI_z & \frac{6}{l^2}EI_z & 0 & 0 & 0 & 0 \\ -\frac{6}{l^2}EI_z & \frac{2}{l}EI_z & 0 & 0 & 0 & 0 \\ 0 & 0 & -\frac{12}{l^3}EI_y & \frac{6}{l^2}EI_y & 0 & 0 \\ 0 & 0 & -\frac{6}{l^2}EI_y & \frac{2}{l}EI_y & 0 & 0 \\ 0 & 0 & 0 & 0 & -\frac{1}{l}GI_x - \frac{1}{l}GI_\beta & \frac{1}{2}GI_\beta \\ 0 & 0 & 0 & 0 & -\frac{1}{2}GI_\beta & \frac{l}{6}GI_\beta - \frac{1}{l}EI_\omega \end{pmatrix},$$

$$K_{21} = \begin{pmatrix} -\frac{12}{l^3}EI_z & -\frac{6}{l^2}EI_z & 0 & 0 & 0 & 0 \\ \frac{6}{l^2}EI_z & \frac{2}{l}EI_z & 0 & 0 & 0 & 0 \\ 0 & 0 & -\frac{12}{l^3}EI_y & -\frac{6}{l^2}EI_y & 0 & 0 \\ 0 & 0 & \frac{6}{l^2}EI_y & \frac{2}{l}EI_y & 0 & 0 \\ 0 & 0 & 0 & 0 & -\frac{1}{l}GI_x - \frac{1}{l}GI_\beta & -\frac{1}{2}GI_\beta \\ 0 & 0 & 0 & 0 & \frac{1}{2}GI_\beta & \frac{l}{6}GI_\beta - \frac{1}{l}EI_\omega \end{pmatrix},$$

$$K_{22}=\begin{pmatrix} \frac{12}{l^3}EI_z & -\frac{6}{l^2}EI_z & 0 & 0 & 0 & 0 \\ -\frac{6}{l^2}EI_z & \frac{4}{l}EI_z & 0 & 0 & 0 & 0 \\ 0 & 0 & \frac{12}{l^3}EI_y & -\frac{6}{l^2}EI_y & 0 & 0 \\ 0 & 0 & -\frac{6}{l^2}EI_y & \frac{4}{l}EI_y & 0 & 0 \\ 0 & 0 & 0 & 0 & \frac{1}{l}GI_x+\frac{1}{l}GI_\beta & -\frac{1}{2}GI_\beta \\ 0 & 0 & 0 & 0 & -\frac{1}{2}GI_\beta & \frac{l}{3}GI_\beta+\frac{1}{l}EI_\omega \end{pmatrix},$$

$$G_{11}=\begin{pmatrix} \frac{6}{5l} & \frac{1}{10} & 0 & 0 & \frac{1}{l}(z_p-e_z) & 0 \\ \frac{1}{10} & \frac{2l}{15} & 0 & 0 & z_p\text{-}e_z & 0 \\ 0 & 0 & \frac{6}{5l} & \frac{1}{10} & \frac{1}{l}(e_y-y_p) & 0 \\ 0 & 0 & \frac{1}{10} & \frac{2l}{15} & e_y-y_p & 0 \\ \frac{1}{l}(z_p-e_z) & z_p-e_z & \frac{1}{l}(e_y-y_p) & e_y-y_p & \frac{1}{l}(r_p^2+e_zb_z+e_yb_y+\omega_Ab_\omega) & 0 \\ 0 & 0 & 0 & 0 & 0 & 0 \end{pmatrix},$$

$$G_{12}=\begin{pmatrix} -\frac{6}{5l} & \frac{1}{10} & 0 & 0 & \frac{1}{l}(e_z-z_p) & 0 \\ -\frac{1}{10} & -\frac{l}{30} & 0 & 0 & 0 & 0 \\ 0 & 0 & -\frac{6}{5l} & \frac{1}{10} & \frac{1}{l}(y_p-e_y) & 0 \\ 0 & 0 & -\frac{1}{10} & -\frac{l}{30} & 0 & 0 \\ \frac{1}{l}(e_z-z_p) & 0 & \frac{1}{l}(y_p-e_y) & 0 & -\frac{1}{l}(r_p^2+e_zb_z+e_yb_y+\omega_Ab_\omega) & 0 \\ 0 & 0 & 0 & 0 & 0 & 0 \end{pmatrix},$$

$$G_{21}=\begin{pmatrix} -\frac{6}{5l} & -\frac{1}{10} & 0 & 0 & \frac{1}{l}(e_z-z_p) & 0 \\ \frac{1}{10} & -\frac{l}{30} & 0 & 0 & 0 & 0 \\ 0 & 0 & -\frac{6}{5l} & -\frac{1}{10} & \frac{1}{l}(y_p-e_y) & 0 \\ 0 & 0 & \frac{1}{10} & -\frac{l}{30} & 0 & 0 \\ \frac{1}{l}(e_z-z_p) & 0 & \frac{1}{l}(y_p-e_y) & 0 & -\frac{1}{l}(r_p^2+e_zb_z+e_yb_y+\omega_Ab_\omega) & 0 \\ 0 & 0 & 0 & 0 & 0 & 0 \end{pmatrix},$$

$$G_{22} = \begin{pmatrix} \frac{6}{5l} & -\frac{1}{10} & 0 & 0 & \frac{1}{l}(z_p - e_z) & 0 \\ -\frac{1}{10} & \frac{2l}{15} & 0 & 0 & e_z - z_p & 0 \\ 0 & 0 & \frac{6}{5l} & -\frac{1}{10} & \frac{1}{l}(e_y - y_p) & 0 \\ 0 & 0 & -\frac{1}{10} & \frac{2l}{15} & y_p - e_y & 0 \\ \frac{1}{l}(z_p - e_z) & e_z - z_p & \frac{1}{l}(e_y - y_p) & y_p - e_y & \frac{1}{l}(r_p^2 + e_z b_z + e_y b_y + \omega_A b_\omega) & 0 \\ 0 & 0 & 0 & 0 & 0 & 0 \end{pmatrix}.$$

3. Results and Discussion

Let us consider a bar with the length L = 5 m with three different types of the cross section: a U-section, cross and rectangular pipe. The bar ends are hingedly supported $(\eta = \zeta = 0;\ \theta = 0)$. A concentrated force P is applied sequentially to two points 1 and 2 of each cross section (Figure 2). To determine the value of the force P with FEM, the stiffness matrix $[K]$ and the geometrical stiffness matrix $[G]$ from the equation (36) are used.

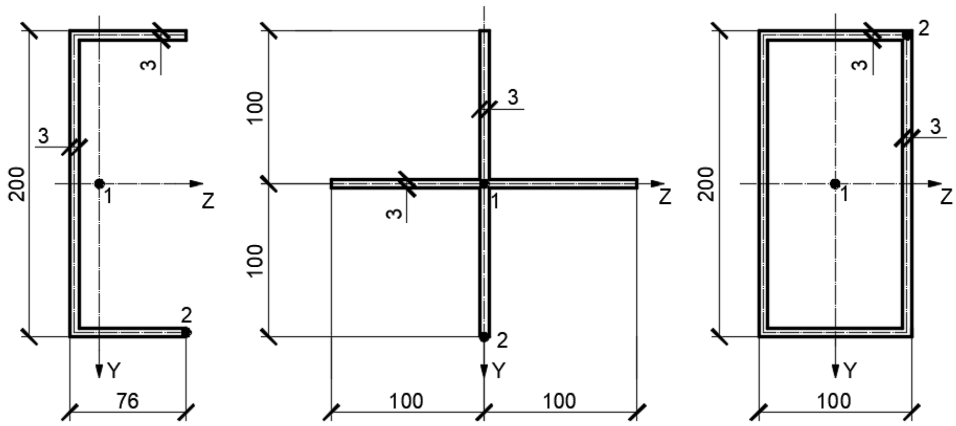

Figure 2. Cross sections of the rod.

The bar is made of steel S245:

$$E = 20600\ \text{kN/cm}^2, \quad G = 7920\ \text{kN/cm}^2.$$

Geometrical data of the cross sections is:

1) For the U-section

$$I_z = 625\ \text{cm}^4,\ I_y = 99\ \text{cm}^4,\ I_x = 0.3\ \text{cm}^4,\ I_\omega = 5139\ \text{cm}^6,\ I_\beta = 564\ \text{cm}^4,\ y_p = 0,$$

$$z_p = -4.2\ \text{cm},\ r_p^2 = 87\ \text{cm}^2,\ b_y = b_\omega = 0,\ b_z = 11.7\ \text{cm}.$$

2) For the cross

$$I_z = I_y = 200\ \text{cm}^4,\ I_x = 0.36\ \text{cm}^4,\ I_\omega = 0,\ I_\beta = 0,\ y_p = z_p = 0,$$

$$r_p^2 = 34\ \text{cm}^2,\ b_y = b_\omega = b_z = 0.$$

3) For the rectangular pipe:

$$I_z = 947\ \text{cm}^4,\ I_y = 324\ \text{cm}^4,\ I_x = 745\ \text{cm}^4,\ I_\omega = 1553\ \text{cm}^6,\ I_\beta = 78\ \text{cm}^4,\ y_p = z_p = 0,$$

$$r_p^2 = 72\ \text{cm}^2,\ b_y = b_\omega = b_z = 0.$$

It is necessary to check the slenderness ratio λ which should be bigger than the critical slenderness λ_{cr}.

Slenderness ratio and the critical slenderness can be found out as follows:

$$\lambda = \frac{\mu L}{i}, \quad \lambda_{cr} = \sqrt{\frac{\pi^2 E}{\sigma_{pr}}},$$

where μ is effective length factor which is $\mu =$ 1 for the bar with both ends hingedly supported;

i is the smallest radius of gyration;

σ_{pr} is limit of proportionality, which is σ_{pr} = 19.5 kN/cm^2 for steel S245;

The critical slenderness is λ_{cr} = 102.

The slenderness ratio for hingedly supported beam is:

1) U-section: $\lambda_h = 161$,

2) cross: $\lambda_h = 122$,

3) rectangular pipe: $\lambda_h = 116$.

In each case slenderness ratio is greater than the critical slenderness.

Solving the basic equation for the bar in compression:

$$\det([K] - P[G]) = 0 \tag{37}$$

we can determine the least root of the equation, which is the critical load P.

Let us compare the critical load values obtained by the equation (37) with the Euler buckling loads and critical load values determined by Slivker's analytical equation for the bar with both ends pinned [20]:

$$\begin{vmatrix} EI_z k^2 + N & 0 & -M_\eta & 0 \\ 0 & EI_y k^2 + N & M_\zeta & 0 \\ -M_\eta & M_\zeta & GI_x + GI_\beta + K & -\dfrac{GI_\beta}{k} \\ 0 & 0 & -\dfrac{GI_\beta}{k} & EI_\omega + \dfrac{GI_\beta}{k^2} \end{vmatrix} = 0, \tag{38}$$

where

$$k = \frac{\pi}{l}.$$

Table 1 shows the critical loads calculated with the equations (37), (38) and Euler buckling loads.

Table 1. Comparison of the critical loads by equations (37), (38) and Euler buckling loads.

Type of the cross section	Critical load		
	FEM	Slivker's analytical equation	Euler buckling load
U-section, point 1	73.5 kN	73.5 kN	80.5 kN
U-section, point 2	30.3 kN	30.3 kN	80.5 kN
cross, point 1	84.9 kN	84.9 kN	162.7 kN
cross, point 2	41.8 kN	41.8 kN	162.7 kN
rectangular pipe, point 1	263.4 kN	263.4 kN	263.5 kN
rectangular pipe, point 2	262.3 kN	262.3 kN	263.5 kN

Let us show the convergence of the FEM solution to the analytical solution for one of the cases: U-section, point 2 (Figure 3). For the other cases the graphs are similar.

The results in Table 1 showed that taking warping into account reduces the critical load for the open cross sections (U-section and cross) but doesn't have a significant impact on the closed cross-section (rectangular pipe).

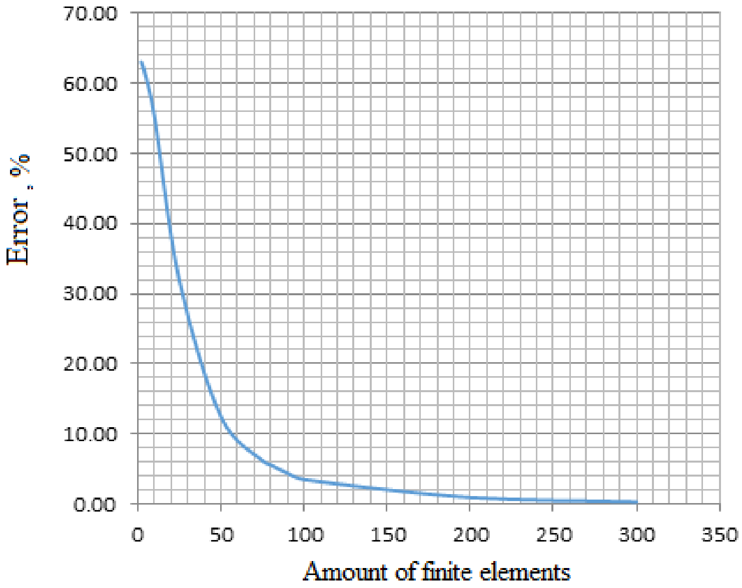

Figure 3. Graph of the convergence of the FEM solution to analytical solution for the case U-section, point 2.

4. Conclusions

1. The geometrical stiffness matrix of the thin-walled finite element within the Slivker semi-shear theory was worked out in this paper. Transverse displacements were approximated with cubical functions while torsion and warping with linear functions.

2. With the constructed matrix, using FEM the critical load was determined for the bar with both ends hingedly supported and different types of the cross section (U-section, cross and the rectangular pipe).

3. The critical load values were also compared with the Euler buckling loads. The results showed that taking warping into account reduces the critical load for the open cross sections (U-section and cross) but doesn't have a significant impact on the closed cross-section (rectangular pipe).

4. The constructed geometrical stiffness matrix is acceptable to solve buckling problems of the thin-walled bars for both open and closed cross sections.

5. As the number of finite elements increases, the numerical solution converges to the exact one.

Finally, it was showed that thickness of the rods sections can lead to a significant decrease of the critical force for the open profile rod (up to 100 %), especially for non-centered compressive force.

References

1. Pavlenko, A.D., Rybakov, V.A., Pikht, A.V., Mikhailov, E.S. Non-uniform torsion of thin-walled open-section multi-span beams. Magazine of Civil Engineering. 2016. 67(7). Pp. 55–69. doi: 10.5862/MCE.67.6
2. Rybakov, V.A., Al, Ali M., Panteleev, A.P., Fedotova, K.A., Smirnov, A.V. Bearing capacity of rafter systems made of steel thin-walled structures in attic roofs. Magazine of Civil Engineering. 2017. No. 8(76). Pp. 28–39. doi: 10.18720/MCE.76.3
3. Vatin, N.I., Nazmeeva, T., Guslinscky, R. Problems of cold-bent notched c-shaped profile members. Advanced Materials Research. 2014. No. 941–944. Pp. 1871–1875.
4. Lalin, V.V., Zdanchuk, E.V., Kushova, D.A., Rosin, L.A. Variational formulations for non-linear problems with independent rotational degrees of freedom. Magazine of Civil Engineering. 2015. 56(4). Pp. 54–65. doi: 10.5862/MCE.56.7
5. Chen, C.H., Zhu, Y.F., Yao, Y., Huang, Y. The finite elements model research of the pre-twisted thin-walled beam. Structural engineering and mechanics. 2016. No. 57. Pp. 389–402.
6. Tusnin, A. Finite element for calculation of structures made of thin-walled open profile rods. Procedia Engineering 2 Cep: 2nd International Conference on Industrial Engineering, ICIE. 2016. Pp. 1673–1679.
7. Kotelko, M., Lis, P., Macdonald, M. Load capacity probabilistic sensitivity analysis of thin-walled beams. Thin-walled Structures. 2017. No. 115. Pp. 142–153.
8. Lanc, D., Turkalj, G., Vo, T.P., Lee, J. Buckling analysis of thin-walled functionality graded sandwich box beams. Thin-walled Structures. 2015. No. 86. Pp. 148–156.
9. Garifullin, M.R., Barabash, A.V., Naumova, E.A., Zhuvak, O.V., Jokinen, T., Heinisuo, M. Surrogate modeling for initial rotational stiffness of welded tubular joints. Magazine of Civil Engineering. 2016. 63(3). Pp. 53–76. doi: 10.5862/MCE.63.4

10. Bely, G.I. Metody rascheta sterzhnevyh ehlementov konstrukcij iz tonkostennyh holodnognutyh profilej [Methods for calculating the rod from thin-walled cold-formed profiles]. Vestnik grazhdanskih inzhenerov. 2014. No. 4 (45). Pp. 32–37. (rus)
11. Bely, G.I. Osobennosti raboty sterzhnevyh ehlementov konstrukcij iz ocinkovannyh gnutyh profilej [Features of the work of structures from galvanized bent profiles]. Vestnik grazhdanskih inzhenerov. 2012. No. 3. Pp. 99–103. (rus)
12. Pesec, O., Melcher, J. Lateral-Torsional Buckling of Laminated Structural Glass Beams. Experimental Study. Procedia Engineering. 2017. No. 190. Pp. 70–77.
13. Tusnin, A.R., Prokic, M. Experimental research of I-beams under bending and torsion actions. Magazine of Civil Engineering. 2015. 53(1). Pp. 24–31. doi: 10.5862/MCE.53.3
14. Nazmeeva, T.V., Vatin, N.I. Numerical investigations of notched c-profile compressed members with initial imperfections. Magazine of Civil Engineering. 2016. 62(2). Pp. 92–101. doi: 10.5862/MCE.62.9
15. Atavin, I.V., Melnikov, B.E., Semenov, A.S., Chernysheva, N.V., Yakovleva, E.L. Influence of stiffness of node on stability and strength of thin-walled structure. Magazine of Civil Engineering. 2018. 80(4). Pp. 48–61. doi: 10.18720/MCE.80.5
16. Tusnin, A.R., Tusnina, O.A. numerical analysis of rod systems behavior after buckling. Procedia Engineering. 2016. No. 153. Pp. 791–798.
17. Jian, L., Yun, T., Yumei, L. Stiffness Matrix of Nonlinear FEM Equilibrium Equation. Procedia Engineering. 2012. No. 29. Pp. 3698–3702.
18. Magnucki, K., Milecki, S. Elastic buckling of a thin-walled rectangular frame under in-plane compression. Thin-Walled Structures. 2017. No. 116. Pp. 326–332.
19. Batista, M. On stability of elastic rod planar equilibrium configurations. International Journal of Solids and Structures. 2015. No. 72. Pp. 144–152.
20. Sastry, S.Y.B., Krishna, Y., Koduganti, A. Flexural buckling analysis of thin walled lipped channel cross section beams with variable geometry. International Journal of Innovative Research in Science, Engineering and Technology. 2014. No. 3(6). Pp. 13484–13494.
21. Trouncer, A.N., Rasmussen, K.J.R. Flexural–torsional buckling of ultra light-gauge steel storage rack uprights. Thin-Walled Structures. 2014. No. 81. Pp. 159–174.
22. Kraav, T., Kraav, T., Lellep, J. Elastic stability of uniform and hollow columns. Procedia Engineering. 2017. No. 172. Pp. 570–577.
23. Mario, M., Giles, W. Column buckling with shear deformation – a hyperelastic formulation. International Journal of Solids and Structures. 2008. No. 45. Pp. 4322–4339.
24. Banan, M., Karami, G. Farshad, M. Finite element stability analysis of curved beams on elastic foundation. Mathematical and Computer Modelling. 1990. No. 14. Pp. 863–867.
25. Hsiao, K., Wen, Y., Chen, R. Geometrically nonlinear dynamic analysis of thin-walled beams. Proceeding of the worldcongress on engineering. 2009. No. 2. Pp. 124–139.
26. Lalin, V., Rybakov, V., Sergey, A. The finite elements for design of frame of thin-walled beams. Applied Mechanics and Materials. 2014. No. 578–579. Pp. 858–863.
27. Dyakov, S.F. Sravnitelnyj analiz zadachi krucheniya tonkostennogo sterzhnya po modelyam Vlasova i Slivkera [Comparative analysis of the problem of torsion of a thin-walled rod according to the models of Vlasov and Slivker]. Stroitelnaya mekhanika inzhenernyh konstrukcij i sooruzhenij. 2013. No. 1. Pp. 24–31. (rus)
28. Derevyankin, D.V., Slivker, V.I. O konechnoehlementnyh approksimaciyah v zadachah ustojchivosti sterzhnej Timoshenko [On finite element approximations in problems of stability of rods of Tymoshenko]. Vestnik grazhdanskih inzhenerov. 2008. No. 4(17). Pp. 17–26. (rus)

Contacts:

Vladimir Lalin, +79213199878; vllalin@yandex.ru
Vladimir Rybakov, +79643312915; fishermanoff@mail.ru
Stanislav Diakov, +79213008917; stass.f.dyakov@gmail.com
Vadim Kudinov, +79618037320; vadim.russia@hotmail.com
Ekaterina Orlova, +79312997098; ye-cat-erina@yandex.ru

Инженерно-строительный журнал

ISSN 2071-0305

сайт журнала: http://engstroy.spbstu.ru/

DOI: 10.18720/MCE.87.6

Полусдвиговая теория В.И. Сливкера в задачах устойчивости тонкостенных стержней

В.В. Лалин, В.А. Рыбаков, С.Ф. Дьяков, В.В. Кудинов, Е.С. Орлова*,
Санкт-Петербургский политехнический университет Петра Великого, Санкт-Петербург, Россия
** E-mail: ye-cat-erina@yandex.ru*

Ключевые слова: устойчивость, геометрическая матрица жесткости, тонкостенный стержень, метод конечных элементов, полусдвиговая теория.

Аннотация. Теория тонкостенных стержней приобрела большую важность в связи с широким использованием легких стальных тонкостенных конструкций. Традиционно, при расчете тонкостенных стержней используют две разные теории: для стержней открытого профиля и стержней замкнутого профиля. При решении задач методом конечных элементов это неудобно, так как приходится строить разные конечные элементы для разных стержней. В 2005 г. В.И. Сливкером была разработана полусдвиговая теория расчета тонкостенных стержней, которая позволяет единым образом решать задачи как для стержней открытого, так и замкнутого профилей. В рамках этой теории в данной работе исследовано применение метода конечных элементов для решения задач устойчивости тонкостенных стержней и построена геометрическая матрица жесткости. Показано, что построенное конечно-элементное решение сходится к точному при увеличении количества конечных элементов. Проведено сравнение полученных решений с критическими силами, вычисленными по классической формуле Эйлера. Сделан вывод о том, что учет тонкостенности сечения может привести к значительному уменьшению критических сил, особенно для стержней открытого профиля.

Литература

1. Павленко А.Д., Рыбаков В.А., Пихт А.В., Михайлов Е.С. Стесненное кручение многопролетных тонкостенных балок открытого профиля // Инженерно-строительный журнал. 2016. № 7(67). С. 55–69. doi: 10.5862/MCE.67.6
2. Рыбаков В.А., Ал Али М., Пантелеев А.П., Федотова К.А., Смирнов А.В. Несущая способность стропильной системы из стальных тонкостенных конструкций в чердачных крышах // Инженерно-строительный журнал. 2017. 76(8). С. 28–39. doi: 10.18720/MCE.76.3
3. Vatin N.I., Nazmeeva T., Guslinscky R. Problems of cold-bent notched c-shaped profile members // Advanced Materials Research. 2014. No. 941-944. Pp. 1871–1875.
4. Лалин В.В., Зданчук Е.В., Кушова Д.А., Розин Л.А. Вариационные постановки нелинейных задач с независимыми вращательными степенями свободы // Инженерно-строительный журнал. 2015. № 4(56). С. 54–65. doi: 10.5862/MCE.56.7
5. Chen C.H., Zhu Y.F., Yao Y., Huang Y. The finite elements model research of the pre-twisted thin-walled beam // Structural engineering and mechanics. 2016. No. 3. Pp. 389–402.
6. Tusnin A. Finite element for calculation of structures made of thin-walled open profile rods // Procedia Engineering 2 Cep: 2nd International Conference on Industrial Engineering, ICIE. 2016. Pp. 1673–1679.
7. Kotelko M., Lis P., Macdonald M. Load capacity probabilistic sensitivity analysis of thin-walled beams // Thin-walled structures. 2017. No. 115. Pp. 142–153.
8. Lanc D., Turkalj G., Vo T.P., Lee J. Buckling analysis of thin-walled functionality graded sandwich box beams // Thin-walled structures. 2015. No. 86. Pp. 148–156.
9. Гарифуллин М.Р., Барабаш А.В., Наумова Е.А., Жувак О.В., Йокинен Т., Хейнисуо М. Суррогатное моделирование для определения начальной жесткости вращения сварных трубчатых соединений // Инженерно-строительный журнал. 2016. № 3(63). С. 53–76. doi: 10.5862/MCE.63.4
10. Белый Г.И. Методы расчета стержневых элементов конструкций из тонкостенных холодногнутых профилей // Вестник гражданских инженеров. 2014. № 4(45). С. 32–37.
11. Белый Г.И. Особенности работы стержневых элементов конструкций из оцинкованных гнутых профилей // Вестник гражданских инженеров. 2012. № 3. С. 99–103.
12. Pesec O., Melcher J. Lateral-Torsional Buckling of Laminated Structural Glass Beams. Experimental Study // Procedia Engineering. 2017. No. 190. Pp. 70–77.
13. Туснин А.Р., Прокич М. Экспериментальные исследования работы балок двутаврового сечения при действии изгиба и кручения // Инженерно-строительный журнал. 2015. № 1(53). С. 24–31. doi: 10.5862/MCE.53.3

14. Назмеева Т.В., Ватин Н.И. Численные исследования сжатых элементов из холодногнутого просечного С-профиля с учетом начальных несовершенств // Инженерно-строительный журнал. 2016. № 2(62). С. 92–101. doi: 10.5862/MCE.62.9
15. Атавин И.В., Мельников Б.Е., Семенов А.С., Чернышева Н.В., Яковлева Е.Л. Влияние жесткости узловых соединений на устойчивость и прочность тонкостенных конструкций // Инженерно-строительный журнал. 2018. № 4(80). С. 48–61. doi: 10.18720/MCE.80.5
16. Tusnin A.R., Tusnina O.A. numerical analysis of rod systems behavior after buckling // Procedia Engineering. 2016. No. 153. Pp. 791–798.
17. Jian L., Yun T., Yumei L. Stiffness Matrix of Nonlinear FEM Equilibrium Equation // Procedia Engineering. 2012. No. 29. Pp. 3698–3702.
18. Magnucki K., Milecki S. Elastic buckling of a thin-walled rectangular frame under in-plane compression // Thin-Walled Structures. 2017. No. 116. Pp. 326–332.
19. Batista M. On stability of elastic rod planar equilibrium configurations // International Journal of Solids and Structures. 2015. No. 72. Pp. 144–152.
20. Sastry S.Y.B., Krishna Y., Koduganti A. Flexural buckling analysis of thin walled lipped channel cross section beams with variable geometry // International Journal of Innovative Research in Science, Engineering and Technology. 2014. No. 3(6). Pp. 13484–13494.
21. Trouncer A.N., Rasmussen K.J.R. Flexural–torsional buckling of ultra light-gauge steel storage rack uprights // Thin-Walled Structures. 2014. No. 81. Pp. 159–174.
22. Kraav T., Kraav T., Lellep J. Elastic stability of uniform and hollow columns // Procedia Engineering. 2017. No. 172. Pp. 570–577.
23. Mario M., Giles W. Column buckling with shear deformation – a hyperelastic formulation // International Journal of Solids and Structures. 2008. No. 45. Pp. 4322–4339.
24. Banan M., Karami G. Farshad M. Finite element stability analysis of curved beams on elastic foundation // Mathematical and Computer Modelling. 1990. No. 14. Pp. 863–867.
25. Hsiao K., Wen Y., Chen R. Geometrically nonlinear dynamic analysis of thin-walled beams // Proceeding of the worldcongress on engineering. 2009. No. 2. Pp. 124–139.
26. Lalin V., Rybakov V., Sergey A. The finite elements for design of frame of thin-walled beams // Applied Mechanics and Materials. 2014. No. 578-579. Pp. 858–863.
27. Дьяков С.Ф. Сравнительный анализ задачи кручения тонкостенного стержня по моделям Власова и Сливкера // Строительная механика инженерных конструкций и сооружений. 2013. № 1. С. 24–31.
29. Деревянкин Д.В., Сливкер В.И. О конечноэлементных аппроксимациях в задачах устойчивости стержней Тимошенко // Вестник гражданских инженеров. 2008. № 4(17). С. 17–26.

Контактные данные:

Владимир Владимирович Лалин, +79213199878; эл. почта: vllalin@yandex.ru
Владимир Александрович Рыбаков, +79643312915; эл. почта: fishermanoff@mail.ru
Станислав Федорович Дьяков, +79213008917; эл. почта: stass.f.dyakov@gmail.com
Вадим Викторович Кудинов, +79618037320; эл. почта: vadim.russia@hotmail.com
Екатерина Сергеевна Орлова, +79312997098; эл. почта: ye-cat-erina@yandex.ru